Investigating the Amyloidogenic Nanostructured Sequences of Elastin: Sequence Encoded by Exon 28 of Human Tropoelastin Gene

Brigida Bochicchio, Antonietta Pepe, Roberta Flamia, Marina Lorusso, and Antonio M. Tamburro*

Department of Chemistry, Università della Basilicata, Via N. Sauro, 85, 85100 Potenza, Italy

Received June 7, 2007; Revised Manuscript Received August 17, 2007

In this paper we demonstrate that the sequence encoded by exon 28 (EX28) of human tropoelastin gene is able to give amyloid-like fibrils. CD (circular dichroism) in solution and solid-state FTIR (Fourier transform infrared spectroscopy) spectroscopies have shown the presence of β-sheet conformation. At the supramolecular level the fibers formed by EX28 peptide were investigated by AFM (atomic force microscopy) and ESEM (environmental scanning electron microscopy). A very big left-handed helix, 100 μm long, is visible together with aggregates of different sizes, some of them being constituted by helically interwoven fibers. Furthermore, an additional AFM image of EX28 is shown where the ultrastructure found is somewhat reminiscent of a more or less retiform film. These findings should be useful for designing proper elastin-inspired biomaterials.

Elastin is well-known for conferring elasticity to tissues and organs such as skin, vascular arteries, and lungs.[1] The elasticity is ensured by the presence of elastic fibers widely studied at supramolecular level. Nowadays, it is accepted that even short amino acid sequences encoded by the gene of human tropoelastin are able to give an ultrastructure very similar if not identical to that exhibited by the entire protein.[2] Although at the supramolecular level elastic fiber structures of different morphology are observed, generally they appear as interwoven, ropelike filaments.[3]

However, some studies have revealed the propensity of some elastin sequences to form also amyloid-like fibers.[4] As a matter of fact, Keeley and co-workers have suggested that elastin sequences rich in proline residues are able to coacervate as elastin does and to give a supramolecular structure very similar to that exhibited by the entire protein. The substitution of the proline amino acids with glycine residues accounts for the irreversible precipitation of the sample from aqueous solution in insoluble fibers characterized at the supramolecular level as amyloid-like.[5]

Originally, the term "amyloid" referred to the protein deposits that accumulate extracellularly in vivo into plaques while, now, it is used for intracellular aggregates and for fibrils deposited in vitro from proteins associated with various diseases ranging from the Alzheimer's dementia (AD) to encephalopathy of Creutzfeldt-Jakob, to Huntington disease (HD), and to type II diabetes. The possible involvement of elastin in amyloid fibrillogenesis and the presence of elastin in arteries such as aortic as well as cerebral opened a new perspective in a potential role of this protein in amyloidogenic diseases.[6]

Beyond this general interest, amyloids have attracted attention for their mechanical properties. Furthermore, fibers derived from elastin sequences could most probably possess also elastic properties; therefore, the self-assembling properties of elastin could be useful for future nanotechnological applications (for a recent review see Rodriguez-Cabello et al.[7]). Short elastin peptides self-assemble into various forms at nanoscale dimensions and therefore they could be useful tools as building blocks for designing nanostructured materials even if some difficulties exist in identifying an appropriate method to ascertain their mechanical properties. Furthermore, although some structural features are common to all amyloid fibrils, the dimension and shape of amyloid aggregates are strongly dependent on the sequences and on the conditions in which fibrillogenesis takes places. As a matter of fact, short polypeptides able to give amyloid fibrils in vitro are also able to form hydrogels useful in biotechnologies such as for drug delivery, release, and tissue engineering. A recent application is based on short peptides with alternating hydrophobic and polar amino acids. In the presence of salt, these form membranes that comprise fibrils with the properties of amyloids. Interestingly, a longer polypeptide such as $(EAK)_9$ forms extremely stable β-sheet structured fibrils, which gel on changing the microenvironment conditions and therefore are called responsive gels. These switchable systems carry additional benefits in drug-delivery and tissue-engineering applications.[8]

To highlight the amyloid-forming propensity of elastin sequences, we have investigated several elastin polypeptide sequences. Until now, we have found that the sequences able to form amyloid fibers are characterized by the presence of the XGGZG motif (X, Z = Val, Leu) as well as by the occurrence of about 20 amino acid residues. As a matter of fact, the sequence encoded by exon 30 (EX30) of the gene of human tropoelastin (GLVGAAG**LGGLGVGGLG**VPG**VGGLG**) as well as the poly(VGGVG) sequences, both containing the XGGZG motif and composed by at least 25 amino acid residues, are able to give amyloid fibers.[5] Interestingly, in the second case the amyloid fibers are formed when deposited from aqueous solvent, differently from what happens in other organic solvents such as methanol, thus calling into question the role of water in determining the amyloid-like behavior of elastin domains. To generalize this hypothesis, we have further investigated the sequence encoded by exon 28 (EX28) of the gene of human tropoelastin (GAAVPG**VLGGLG**A**LGGVG**IPGGVV**)** where

* Corresponding author. Tel.: ++39 0971 202480. Fax: ++39 0971 202223. E-mail: antonio.tamburro@unibas.it.

10.1021/bm700636a CCC: $37.00
Published on Web 10/12/2007

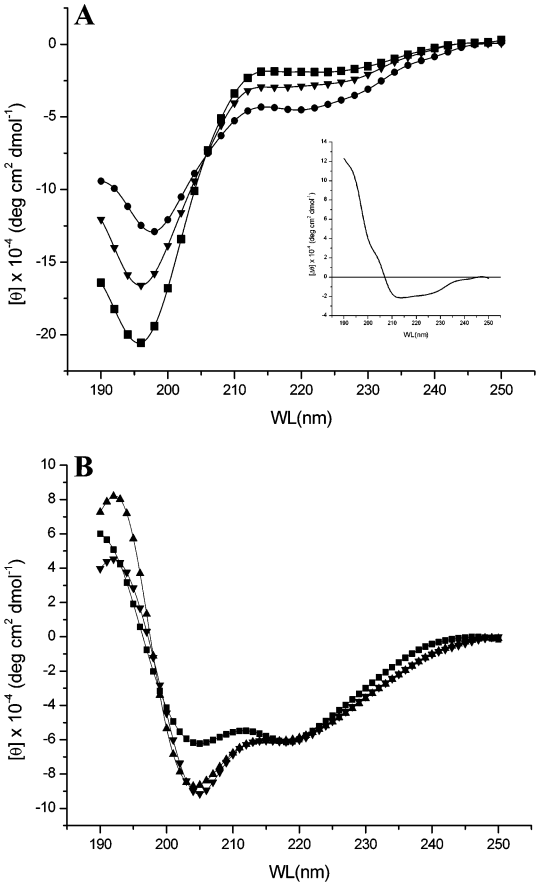

Figure 1. CD spectra of EX28 peptide. (A) In aqueous solution at 0 °C (■), at 25 °C (▼), and at 60 °C (●). Inset: CD difference spectra in aqueous solution of EX28 peptide. The difference spectrum was obtained by subtracting the curve at 0 °C to that at 60 °C.(B) In TFE at 0 °C (■), at 25 °C (▼), and at 60 °C (●).

the XGGZG motif is tandem repeated even if interspersed with an alanine residue.

The techniques used are those commonly accepted to ascertain the presence of amyloid fibers such as UV spectroscopy to verify the binding of the sample to Congo Red and its ability to irreversibly precipitate as a function of temperature. Furthermore, the presence of β-sheet conformation, a condition necessary but not sufficient for amyloid formation, was assessed in solution by CD spectroscopy and in the solid state by FTIR (Fourier transform infrared spectroscopy). These studies were completed by AFM and ESEM measurements for assessing the supramolecular structure of the aggregates that, in the core of amyloids, is constituted by characteristic helical ribbons.

Experimental Section

Peptide Synthesis and Purification. The EX28-coded polypeptide sequence was synthesized by solid-phase methodology using an automatic synthesizer APPLIED BIOSYSTEM model 431 A. Fmoc/DCC/HOBT chemistry was used, starting from 222 mg (0.25 mmol) of Wang resin (Nova Biochem, Laufelfingen, Switzerland). The Fmoc-amino acids were purchased from Nova Biochem (Laufelfingen, Switzerland) and from Inbios (Pozzuoli, Italy). The cleavage of the peptide from resin was achieved by using an aqueous mixture of 95% trifluoroacetic acid. The peptide was lyophilized and purified by reversed-phase HPLC (high-performance liquid chromatography) (see Supporting Information). Binary gradient was used and the solvents were H_2O (0.1% TFA) and CH_3CN (0.1% TFA). The purity of peptide was assessed by electrospray mass spectrometry (see Supporting Information).

Table 1. Assignment of Proton Resonance of Peptide EX28 in TFE-d_3/H_2O (80/20, v/v) at 298 K

	chemical shift of proton resonance (ppm)				
residue	NH	Hα	Hβ	others	$-\Delta\delta/\Delta T$ (ppb/K)
G^1		3.84			
A^2	8.12	4.42	1.42		4.7
A^3	7.81	4.44	1.40		5.3
V^4	7.52	4.49	2.11	γ 0.99	5.3
P^5		4.40	2.30/2.00	γ 2.11/2.002 δ 3.84/3.69	
G^6	7.95	3.87/4.06			
V^7	7.59	4.09	2.18	γ 1.00	3.7
L^8	7.84	4.35	1.70	γ 1.68 δ 0.98	4.9
G^9	7.95	3.86			
G^{10}	7.96	3.95			
L^{11}	7.85	4.33	1.70	γ 1.70 δ 0.94	5.9
G^{12}	8.14	3.92			4.7
A^{13}	7.78	4.32	1.47		4.4
L^{14}	7.77	4.35	1.80	1.71 0.95	4.4
G^{15}	7.93				
G^{16}	7.94	4.00			
V^{17}	7.64	4.18	2.15	γ 0.99	4.4
G^{18}	8.04	3.99/3.92			5.9

CD Spectroscopy. CD spectra for the peptides were obtained using a Jasco J-600 Spectropolarimeter at various temperatures and at concentrations of 0.1 mg/mL in water by using cells of 0.1 cm. Spectra were acquired in the range 190−250 nm by taking points every 0.1 nm, with 20 nm min^{-1} scan rate, an integration time of 2 s, and a 1 nm bandwidth. The data are expressed in terms of [Θ], the molar ellipticity in units of degree cm^2 $dmol^{-1}$.

Nuclear Magnetic Resonance Spectroscopy. All ^1H NMR experiments were performed on a Varian Unity INOVA 500 MHz spectrometer equipped with a 5 mm triple-resonance probe and z-axial gradients. The purified peptide was dissolved in 700 μL of TFE-d_3/H_2O (80/20), containing 0.1 mM of 3-(trimethyl-sily1)-1-propane sulfonic acid (DSS) as internal reference standard at 0 ppm. 3 mM peptide solutions were used. One-dimensional spectra were acquired in Fourier mode with quadrature detection and the water signal was suppressed by a 2.5 s presaturation pulse. Two-dimensional TOCSY[9] and NOESY[10] spectra were collected in the phase-sensitive mode using the States method. Typical data were 2048 complex data points, 16 or 32 transients, and 256 increments. Relaxation delays were set to 2.5 s and spinlock (MLEV-17) mixing time was 80 ms for TOCSY while 100−200 ms mixing time was applied to NOESY experiments. Shifted sine bell squared weighting and zero filling to 2K × 2K was applied before Fourier transformation. The residual HDO signal was suppressed by double-pulsed field-gradient spin−echo.[11] Amide proton temperature coefficients were usually measured from 1D ^1H NMR spectra recorded in 5 °C increments from 20 to 45 °C, while for overlapping resonances a series of TOCSY were recorded to measure the amide temperature coefficients. Spectra were processed and analyzed by VNMR Ver. 6.1C software (Varian, Palo Alto, CA).

Sequential resonance assignments were made by the approach described by Wüthrich.[12] When necessary, to resolve ambiguities arising from chemic al shift degeneracy, spectra were recorded at different temperatures (25 and 40 °C).

Congo Red Binding. A 2 mM solution (1.5 mL) of the EX28 peptide in Tris (50 mM), NaCl (1.5 M), and $CaCl_2$ (1.0 mM) (pH 7.0) solution was incubated overnight at room temperature. The solution was stirred to suspend the precipitated peptide, and an absorbance spectrum from 400 to 600 nm was collected with a Cary UV spectrophotometer using

quartz cuvettes. Congo Red was added to a final concentration of 3.0 M, and the spectrum was recorded. A third spectrum of the unbound dye was also collected. The spectrum of peptide alone was subtracted from the spectrum of Congo Red with peptide to correct for the turbidity of the sample due to the precipitated material.

Turbidimetry Experiments. A 3 mM solution (1.5 mL) of the EX28 peptide in Tris (50 mM), NaCl (1.5 M), and $CaCl_2$ (1.0 mM) (pH 7.0) solution was stirred, to suspend the precipitated peptide. Turbidimetry was measured at 440 nm as a function of temperature on a Cary UV50 spectrophotometer equipped with a Peltier temperature controller using quartz cuvettes and reported as TAA (turbidimetry on apparent absorbance) vs temperature. The temperature solution was increased at rate of 1 °C/min, monitoring the absorbance at that temperature and at 440 nm after 5 min.

FTIR Spectroscopy. EX28 peptide was analyzed by FTIR either as a lyophilized powder or as precipitated fibers in KBr pellets. The spectra were recorded on a Jasco FTIR-460 PLUS using a resolution of 4 cm^{-1} and then smoothed by using the Savintky-Goolay algorithm. The samples were examined at the solid state in KBr pellets (1 mg/100 mg). The decomposition of FTIR spectra was obtained using GRAMS32 software. The percentage of Gaussian and Lorentzian functions was fixed at the 8:2 ratio.

Atomic Force Microscopy. EX28 peptide was solubilized in double-distilled water to a final concentration of 0.5 mg/mL. A first observation was performed by depositing 10 μL of the solution onto silicon coupons taken from a 100 wafer and left to dry at ambient conditions (20−25 °C, atmospheric pressure, ∼50% of humidity). The specimens were then rinsed twice with 200 mL of double-distilled water. Samples were stored sealed in a Petri dish for 1 week and then observed by the scanning force microscope (Procedure A). The second observation was performed after the sample was left for 1 week in the vial and then treated as described above (Procedure B). Experiments were carried out in tapping mode with a NanoScope III Multimode microscope (DI, California), using rectangular-shaped Si cantilevers ("Golden" silicon cantilevers NSG 10, NT-MDT, Russia) with a resonant frequency of about 255 kHz. Typical curvature radius of tips is less than 10 nm.

Environmental Scanning Electron Microscopy. The sample was solubilized in water and evaluated in its hydrated forms on a Philips XL ESEM microscope under a range of controlled pressure between 4.5 and 5.5 Torr without gold sputtering. Gold sputtering was not used because of the presence of steam in the analytical chamber that ensures sample electrical conductivity.

Results

CD Measurements. CD spectroscopy is a useful tool for identifying the global conformation of a peptide or a protein. It is also helpful in highlighting the conformational changes as a function of environmental changes, such as temperature, solvent, salt, and peptide concentration. The CD spectra of a protein can be assumed to be the linear combination of the spectra of the secondary structural elements, so difference spectra of CD spectra recorded in different conditions should point out the conformational changes involved. CD spectra of EX28 peptide were recorded in different solvents and at different temperatures (Figure 1). In aqueous solution (Figure 1A) at 0 °C the CD spectrum shows a trend toward a positive band at about 215 nm and a negative band at about 195 nm. On increase of the temperature to 25 °C and to 60 °C, the zone at 215 nm adopts more negative values while the negative band diminishes in intensity. These spectral features are diagnostic for the presence of the extended PPII helix, in equilibrium with unordered conformations as suggested by the presence of an isodichroic point at about 208 nm. At lower temperatures the CD spectra clearly indicate the presence of PPII conformation.[13] The temperature CD difference spectra between 60 and 0 °C of EX28 in water are shown in Figure 1A (inset). The curve obtained by subtracting the spectra at the two extreme temperatures, 60 and 0 °C, shows a maximum at 202 nm and a minimum at 217 nm. This type of curve is typical of a mixture of β-sheet and unordered conformations and indicates a conformational transition toward the β-sheet conformation on increasing the temperature. In TFE at 0 °C two negative bands of comparable intensities are present at 220 nm and at 203 nm. Furthermore, a strong positive band appears at about 192 nm. The spectrum is only slightly changed at 25 °C where the negative band at 203 nm and the positive one at 192 nm increase moderately. At 60 °C the band at 192 nm increases while the two negative bands remain substantially unchanged. The CD curves in TFE are compatible with the presence of β-turns, either of type I or type II together with unordered conformations.

NMR Studies. The NMR experiments of EX28 peptide were recorded in TFE-d_3/H_2O 80/20 at 25 °C. The 1D proton spectrum shows a high overlap of the amide proton signals in the region 7.5−8.2 ppm (Figure 2). The TOCSY spectra recorded at 60 and 80 ms mixing time confirmed the presence of a crowded region, corresponding to extreme overlap of the 10 glycine residues, which are confined within two spots. The other residues were assigned straightforward by classical peptide assignment strategies (Table 1).

2D TOCSY spectra highlighted also the presence of a minor conformer population, attributed to the *cis*-proline isomers. Nevertheless, the major conformation represents more than 90% and corresponds to the all trans-Pro isomer. The presence of less than 10% of *cis*-Pro isomer in equilibrium with the major *trans*-Pro isomer is common and reflects the low difference in the free energy level of the two isomers and the relatively low-energy barrier ($\Delta G^{\#}$) for isomerization. From a conformational point of view, basically the *cis*-Pro isomer may favor PPI (polyproline I helix) and/or the very rare type VI β-turn, but not the β-strand conformations essential for amyloid formation. As a consequence, to our present knowledge a role for the *cis*-Pro isomer in the amyloid aggregation should be ruled out. Accordingly, the following conformational analysis refers to the major conformer and follows the methods previously carried out for other hydrophobic elastin-related peptides, based on the combined analysis of chemical shift index (CSI), temperature coefficients of amide NH chemical shifts, and the pattern of intra- and inter-residue NOEs.[14]

Chemical shift index analysis is based on the observation that some secondary structures present chemical shift values for some atoms (Hα, Cα, CO) upfield or downfield shifted with respect to random coil values.[15] In particular in ^{1}H NMR spectroscopy CSI is a valuable tool for identifying α-helix and β-sheet by simply comparing the chemical shifts of Hα protons of the residues with the tabulated random coil values, while it is worthless in identifying β-turns or PPII conformations. In the case of EX28 peptide all the Hα proton chemical shifts are in the range of random coil values, thus excluding the presence of α-helix as well as of β-sheet conformations. Also, the NOE data excluded the presence of α-helix, while some NOEs point to the presence of β-turns. In particular, the presence of $d_{\alpha N}$-(i,i+2) connectivities between P_5 and V_7 together with d_{NN}-(i,i+1) NOE connectivities between G_6 and V_7 strongly suggest the presence of a turn in the sequence V_4PGV_7.

Further evidence of the presence of a turn in this region is the low-temperature coefficient ($-\Delta\delta/\Delta T = 3.7$ ppb/K) of V^7, a clear indication that this amide proton is involved in a hydrogen bond. Furthermore, PG units at the corner of β-turns are often present in elastin-related peptides, such as $(VPGVG)_n$,[16]

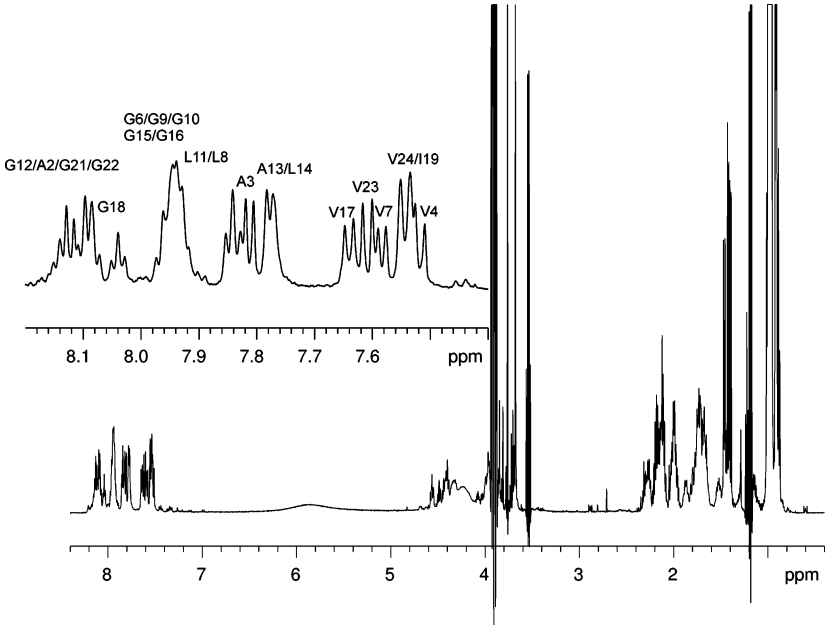

Figure 2. 1D proton NMR spectrum of EX28 recorded in TFE-d_3/H_2O (80/20 v/v) at 298 K. The inset shows the amide region, where the signals are marked with the assigned residues.

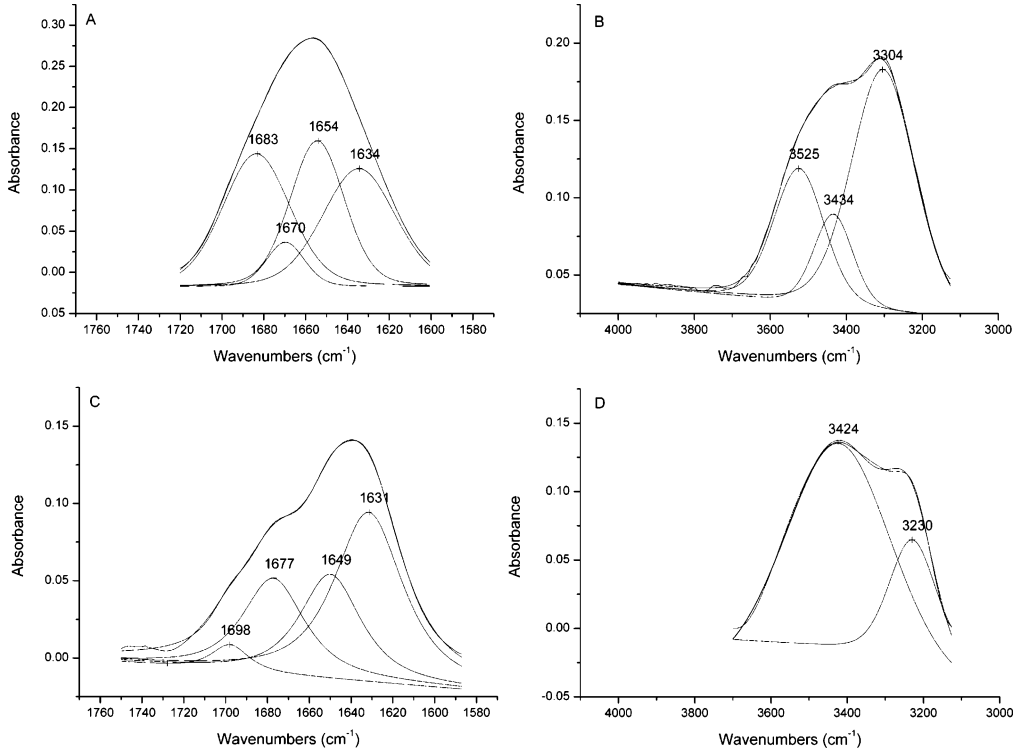

Figure 3. FTIR band separation. (A) Amide I and (B) Amide A regions of lyophilized EX28 peptide in KBr pellet. (C) Amide I and (D) Amide A regions of EX28 fibers in KBr pellet.

or in other hydrophobic domains, such as exon 6-, 9-, 26-, and 30-coded domains of human tropoelastin,[14] where they usually form type II β-turns. The presence of a type II β-turn in the EX28 peptide is confirmed by the following set of NOEs: strong $d_{\alpha N}(i,i+1)$ connectivity between P_5 and G_6, strong $d_{NN}(i,i+1)$ NOE between G_6 and V_7, and the $d_{\alpha}\delta(i,i+1)$ NOEs between V_4 and P_5, confirming the presence of *trans*-Pro isomer.

The temperature coefficients ($-\Delta\delta/\Delta T$) of other amide protons of the EX28 peptides showed values in the range of 4−5 ppb/K. These values are usually attributed to a very weak H-bond or to an equilibrium between turns and other conformations without H-bond. In TFE solution, some relatively low amide protons temperature coefficients ($4 < -\delta\Delta/\delta T < 5$) were measured for residue L_8, G_{12}, A_{13}, L_{14}, V_{17}, and V_{23}, suggesting the presence of some population of turn conformations. Unfortunately, high overlap of the glycine signals precluded the possibility to confirm these β-turns by diagnostic medium-range NOEs.

FTIR Spectra. The band fitting of the FTIR spectrum in the amide I region of lyophilized EX28 peptide is shown in Figure 3A. The amide I region contains a small component at 1670 cm^{-1}, usually assigned to non-hydrogen-bonded groups or

groups weakly bonded to the solvent, normally absorbing at 1666 to 1670 cm^{-1}.[17] In our case, because of the absence of the solvent, the band is assigned to the presence of PPII conformation[18,19] which is an extended helix lacking intramolecular hydrogen bonds.[13,20]

Three main components are present at 1655, 1683, and 1634 cm^{-1}. The component at 1655 cm^{-1} is assigned to unordered conformations and/or to helical conformations.[21] The remaining two bands at 1634 cm^{-1} and at 1683 cm^{-1} are indicative of cross-β and antiparallel β-sheet structures, respectively.[22,23] We propose for the EX28 lyophilized peptide a dominance of unordered and β-structures, while the PPII conformation is of minor contribution. FTIR analysis of the Amide I region of EX28 fibers (Figure 3C) shows a prominent band at 1631 cm^{-1} due to cross-β structures, together with a small band at 1698 cm^{-1}, which is typical of the antiparallel β-sheet conformation. Two minor bands at 1649 and 1677 cm^{-1} could originate from unordered and PPII conformations, respectively. Accordingly, the FTIR data show that the antiparallel β-sheet of the cross-β type is the main structural component of EX28 fibers, whereas in the lyophilized EX28 peptide it is of minor contribution because of the coexistence of PPII and unordered conformations.

The amide A spectra of lyophilized EX28 peptide and EX28 fibers are shown in Figures 3B and 3D, respectively. In Figure 3B one strong band is present at 3304 cm^{-1}, also present in collagen and elastin,[24] which both contain the PPII conformation. Other two bands at 3435 and 3525 cm^{-1} are probably due to hydrogen-bonded and free OH groups of water, respectively. In EX28 fibers the Amide A band appears at surprisingly low wavenumbers, i.e., 3230 cm^{-1}, indicating a possible set of hydrogen-bonded NH groups.

Time-Dependent Fibril Formation and Congo Red Binding. The EX28 peptide (3.0 mM) in Tris buffer (50 mM), NaCl (1.5 M), and $CaCl_2$ (1 mM) (pH 7.0) solution formed a gel-like material after 12 h at room temperature (Figure 4A). The precipitation process is irreversible as demonstrated by the turbidimetry measurements shown in Figure 4B. The formation of viscous material is indicative of the formation of amyloid-like fibrils.[25,26] Congo Red is widely used as an indicator of amyloid deposition. The binding interaction is characterized by both hyperchromic (absorbance increase) and bathochromic (red shift) effects in the absorbance spectrum of the dye.[27] The interaction of EX28 aggregates with Congo Red is shown in Figure 5 and provides additional evidence for the ability of EX28 to self-assemble in amyloid-like structures.

Microscopy Studies. At the supramolecular level, EX28 is able to self-aggregate, giving rise to fibers frequently folded over themselves. (Figure 5). The capability of the EX28 polypeptide sequence to self-aggregate is confirmed by Figure 5 where a very long fiber (the overall length is about 10 μm), obtained according to Procedure A, is shown. In the same image, on the upper right corner, a beaded string is present, and all around the fibers several globules are evident, whose diameter is comparable with that of the fiber. Even though a clear convolution with the tip shape is visible at the left side of the fiber, the amyloid-like internal structure of this fiber is recognizable (Figure 5). At higher magnification (Figure 5), the long fiber appears as composed by right-handed helices with a pitch of about 12.5 nm. The main helix is subdivided into two arms (whose average diameter is about 13 nm), they wound on themselves for a certain length, and then they start to wound together again. Another type of amyloid fiber, with a different supramolecular organization was found, according to Procedure B. A very big left-handed helix, 100 μm long with a pitch

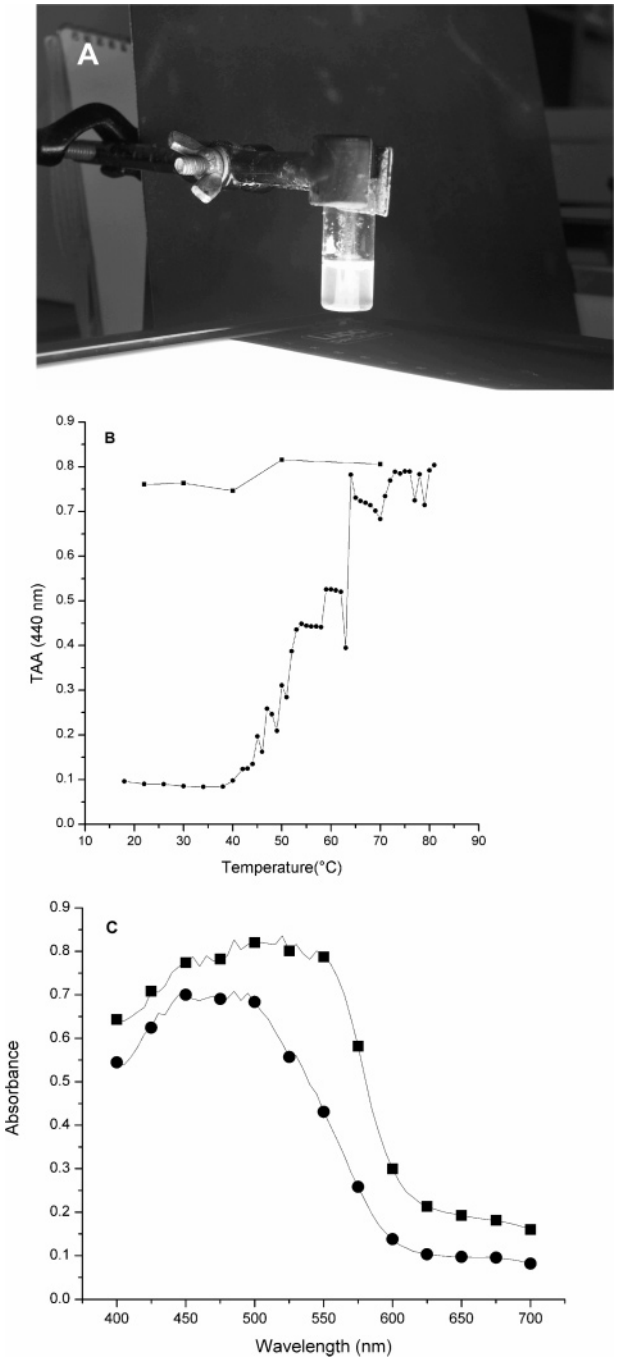

Figure 4. Aggregation and Congo Red binding assay of EX28 peptide. (A) EX28 peptide (3.0 mM) in Tris buffer (50 mM), NaCl (1.5 M), and $CaCl_2$ (1 mM) (pH 7.0) formed a gel-like material after 12 h. (B) Turbidimetry experiment of EX28 peptide (3.0 mM). (●) Warming curve; (■) cooling curve. (C) Affinity of Congo Red to EX28 peptide at room temperature. UV absorption spectrum of Congo Red (●) and of Congo Red bound to EX28 peptide (■).

ranging from 110 to 125 nm and an average diameter of about 185 nm, is visible in Figure 6 together with aggregates of different sizes whose diameters are in the range of 50−100 nm (Figure 6) and where some aggregates are constituted by helically interwoven fibers.

Some of the aggregates are clearly connected with the main fiber (red arrows in the image), suggesting that they could be involved as intermediate in the amyloid-like self-assembly. According to the structural analysis described in Figure 6, a possible pathway for the self-assembly of this amyloid fiber can be proposed: starting from globules of 50 nm (i), the

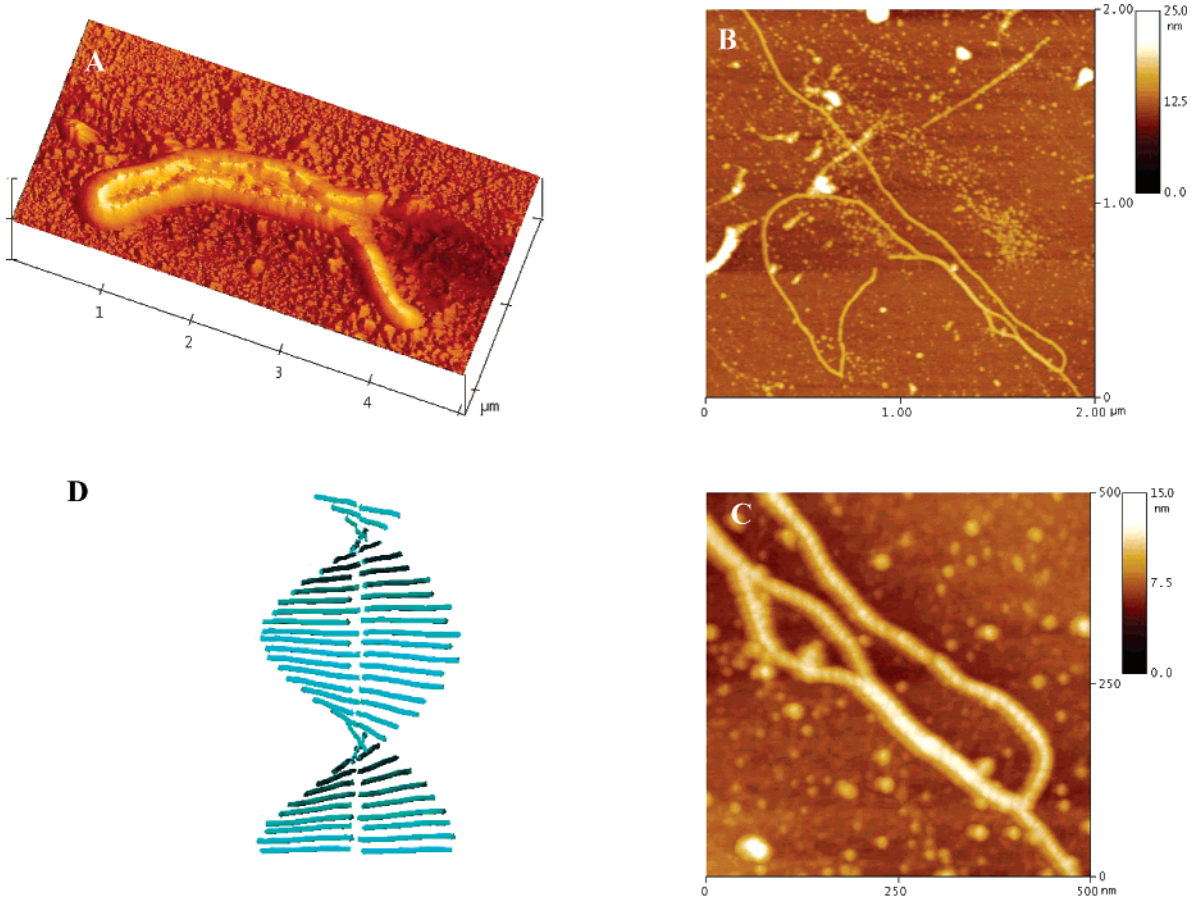

Figure 5. AFM of EX28 peptide. (A) 3D reconstruction of a folded fiber. (B) EX28 peptide forms very long, flexible, twisted rope fibers. (C) At higher magnification the right-handness of the twist is discernible. (D) A schematic model of a possible arrangement in the fiber of EX28 peptide structured in antiparallel β-strands.

following step is represented by two different aggregations of the globules (ii/ii′). When the aggregation occurs in an ordered manner (ii), hierarchical coalescence of the globules is observed (iii), evolving finally to the left-handed rigid helix (iv). As a matter of fact, the in-depth examination of the "final" fiber allows highlighting of the presence of contours reminiscent of the globules, thus confirming their role as an elemental unit of the amyloid fiber assembly.

We note that globular structures are commonly observed as intermediates during the amyloids formation. One could speculate about a unified model linking the molecular structure of EX28 to the helix of Figure 5 and to the globules of Figure 6. The idea follows from the assumption that the superhelix shown in Figure 6B is indeed obtained by globules and aggregates of globules [Figure 6D, pattern (i)−(iv)] while in their turn the helices of Figures 5A−5C derive from the elemental helix whose model is reported in Figure 5D. As a matter of fact, two different models may be proposed. In the first one, the "elemental" globules are formed by several molecules of EX28 which possess an ensemble of conformations, probably in equilibrium among them.[14] Such a situation should possibly lead to spheroidal objects. Actually, in the absence of a preferred direction of interaction (given by single quasi-extended conformations, see the following second model), molecular form should be that dictated by the surface tension acting on hydrophobic systems in an aqueous environment. Of course, the aggregation of molecular globules must give rise to supramolecular globules. The second model favors a direct interaction via β-sheet structured regions of different molecules of EX28, to form the helix shown in Figure 5C. In this case, the intermolecular interactions are shifting the conformational equilibria inside the single molecule of EX28 toward the β-sheet, therefore excluding the possibility of globules formation. NMR studies in the solid state, to be carried out by our laboratory in the very next future, should contribute to clarifying at least some of the above points.

On the whole, the fiber as well as the polymorphous aggregates are constituted by "elemental" globule-like objects, which may be described, in terms of fractal geometry, as products of diffusion-limited aggregation with some preferential direction of growth.[28] As found for several sequences belonging to tropoelastin, the same motif is repeatedly observed at different scales, again an indication of fractal geometry.[25] In this case, the helical motif, typical of amyloid-like fibers, is observed in ESEM (Figure 7) as well as in AFM technique. Furthermore, even in AFM, intertwined fibers are observable at different magnification levels.

Finally, Figure 8 shows an additional AFM image of EX28 where the ultrastructure found is somewhat reminiscent of a more or less retiform film as already found for alpha-elastin[29] and cross-linked poly(OrnGlyGlyOrnGly).[30]

Discussion

The experimental data, reported above, demonstrate that EX28 polypeptide is able to give an irreversible precipitation that depends on some variables such as temperature and time. This precipitate has been shown to be constituted by amyloid-like fibrils. Studies at the molecular level in solution show that EX28

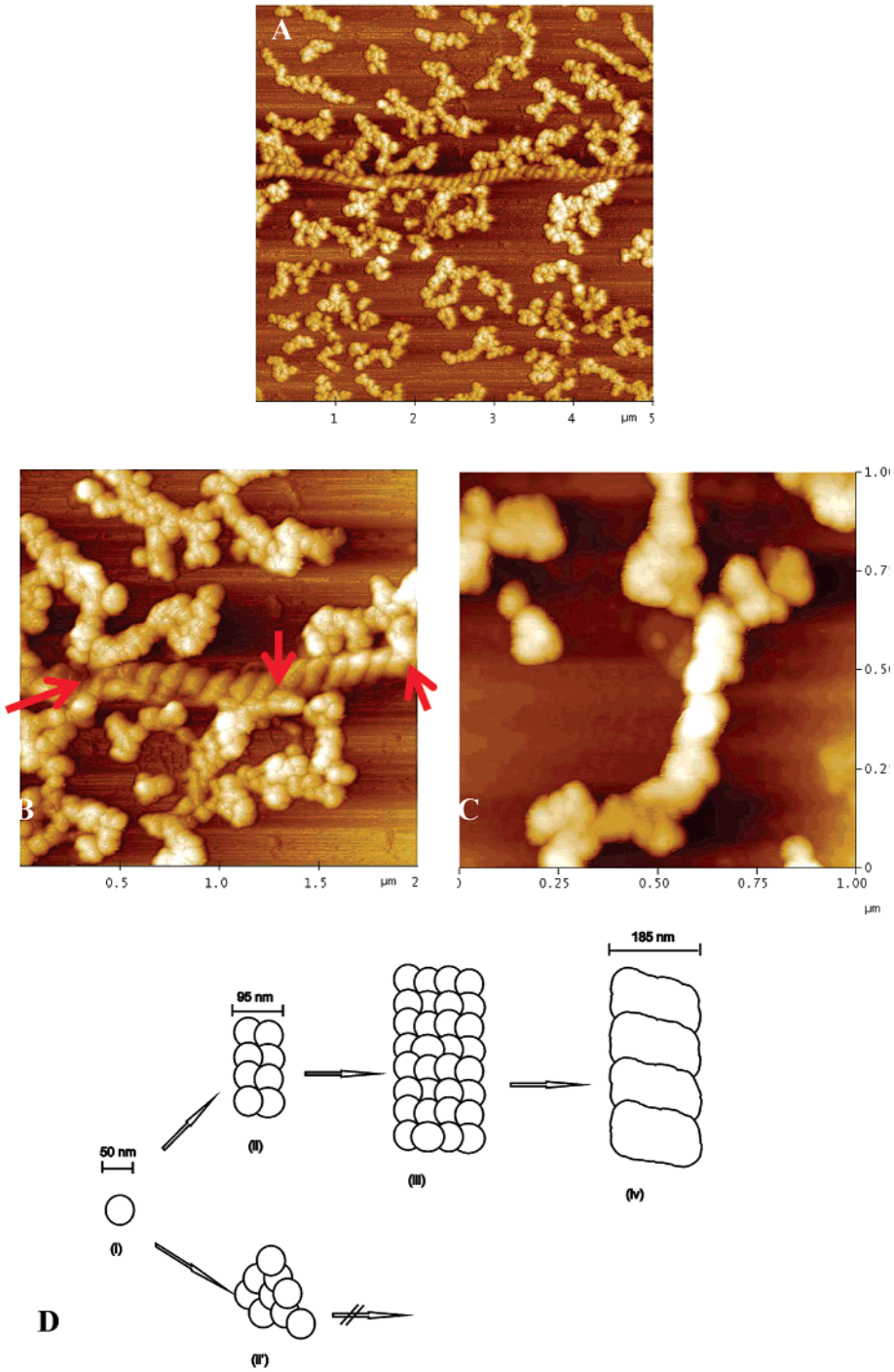

Figure 6. AFM of EX28 peptide. (A) A very long left-handed fiber coexists with polymorphic more or less ordered aggregates. (B) At higher magnification, branches of aggregates connected with the main fiber are evident (red arrows). (C) A potential intermediate aggregate of 85−100 nm of diameter. (D) A possible pathway for EX28 peptide amyloid formation.

adopts a mixture of PPII, β-sheet, and unordered conformations in aqueous solution while β-turns are chiefly found in TFE.[14] This conformation ensemble is typical for all the tropoelastin hydrophobic domains analyzed and, interestingly, has been observed also by solid-state NMR studies of an elastin amyloidogenic polypeptide sequence, containing the XGGZG (X, Z = L,V) motif tandem repeated in EX28, i.e., poly(LGGVG).[31]

Because of their insolubility, structural studies in the solid state are crucial for understanding the amyloid-like nature of the fibers. As previously stated in the Introduction, the role of water is crucial in determining the amyloid-like behavior of some elastin sequences; therefore, the study of the same elastin-derived material at different hydration levels could add new insights for possibly revealing the amyloid fibrillogenesis mechanism common to all amyloidogenic proteins. Within this context, the observation of EX28 fibers coming out from aqueous solution (obviously under conditions of maximal hydration), and of lyophilized powder where water is present in a minimal amount, is worth of note. Accordingly, FTIR studies on both EX28 fibers and EX28 lyophilized have been carried out. These studies showed that the ratio between the conformer populations changes from lyophilized powder to fibers. Indeed, even if the ensemble of conformations found is the same in both samples (i.e., PPII, unordered conformations, and β-sheet), the data suggest the dominance of PPII and of

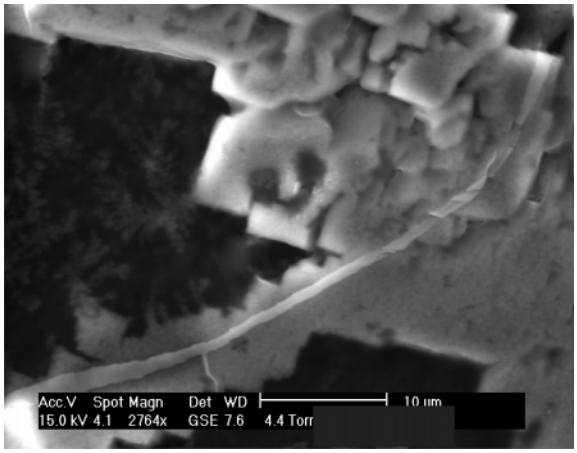

Figure 7. ESEM of EX28 peptide. A very big fiber is shown.

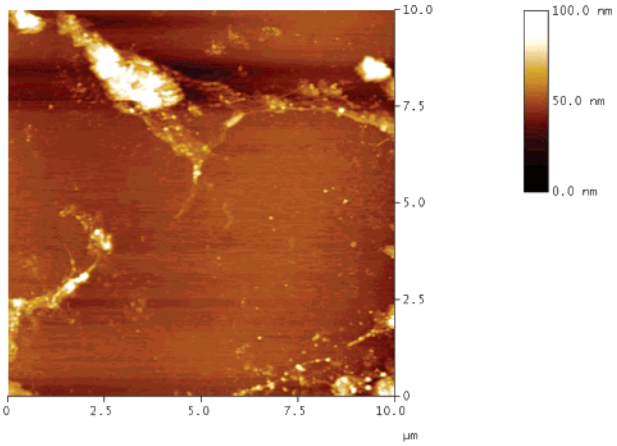

Figure 8. AFM of EX28 peptide showing a delicate network.

unordered conformations in the powder and of antiparallel β-sheets in the fibers.

These findings could be explained by the hypothesis that, in the case of fibers, EX28 polypeptide, which is mainly structured in β-conformation favored at high temperatures, irreversibly precipitates into amyloid fibers by deposition from aqueous solution. This mechanism is not possible by slow lyophilization where water is present at the end only in small amounts, and therefore also the β-structure is not formed and consequently the amyloid fibers are not formed. As a matter of fact, the precipitation is obtained at high temperatures (see turbidimetry experiments) that also favor β-sheet conformation while the lyophilization occurs at low temperatures.

FTIR analysis reveals that in the fibers antiparallel β-sheet chains, probably originating from the cross-β structures, are dominant. The same structural motifs are found also in elastin and lamprin sequences where the GGLGX (X = L,V,Y) motif is recurring.[32] Furthermore, the EX30-coded sequence where the GGLGX motif is tandem repeated has been demonstrated to give amyloid-like fibers.[3] Recent studies have indicated in a combination of electrostatic, polar, and hydrophobic interactions the driving force toward amyloid formation.[33] In the case of elastin, the absence of any charged amino acid residue in EX30, as well as in EX28, suggests that amyloid formation is predominantly driven by hydrophobic interactions favored by increasing the temperature and/or the concentration of the peptide. The final step of this process is the transition toward the β-sheet conformation with concomitant precipitation of the aggregates.

A different, totally reversible self-aggregation process for tropoelastin is the well-known coacervation[34] proposed to promote alignment and cross-linking of tropoelastin molecules.[35,36] At a macroscopic level the protein comes out from the solution as a second phase on increasing the temperature. At the molecular level coacervation promotes the formation of folded conformations, mainly β-turns.[34] Recently, the domains mainly responsible for the coacervation of tropoelastin have been identified as those belonging to the proline-rich domains of human tropoelastin (exons 18, 20, 24, and 26).[37] Interestingly, these domains are unable to form amyloid-like fibrils.[38] In fact, the proline-rich sequences prefer the PPII conformation[13] whose phi_s dihedral angles are frozen at a value (around −70 °C) not compatible with those of the antiparallel β-structure (around −120°). On the other hand, EX30 peptide does not coacervate and gives rise to an irreversible precipitation. At the supramolecular level the coacervation induces the formation of well-ordered filamentous structures,[39] while fibrils characterized by interwoven helices side by side interacting characterize the amyloid of the EX30 sequence. The same supramolecular pattern is shown by the elastin-like biopolymer poly(VGGVG), containing the sequence VGGVG, which is similar to LGGLG and VGGLG spanned by EX30 peptide, that self-assemble in amyloid-like fibers when deposited from aqueous suspensions.[40] As a matter of fact, the motif XGGZG (X, Z = L, V, L, A, I), is widely found in prion protein and in other amyloid-forming proteins such as collagens IV and XVII, fibrillin 2 precursor, flagelliform silk protein, major ampullate gland dragline silk protein, major prion protein precursor, and lamprin precursor and in amyloid β A4 precursor protein-binding family, etc. and is twice repeated in EX28 although interspersed with an alanine residue. Indeed, we have investigated some polypeptide sequences of variable length all containing the XGGZG motif and have demonstrated that the presence of this motif is the "condicio sine qua non", i.e., the necessary but not sufficient condition for the self-aggregation into amyloid fibers (unpublished data). Interestingly, among the polypeptide sequences studied only those containing at least 25 amino acid residues were able to give amyloid-like fibers. As a matter of fact, EX7 polypeptide sequence, a polypeptide composed of only 17 amino acid residues that share with EX30 and EX28 the XGGZG motif once repeated in the EX7 sequence, is unable to give amyloid-like fibrils (data not shown).

Going to the side of nanotechnologies, we have to emphasize that even a so short not cross-linked peptide such as EX28 (only 24 amino acid residues) is nevertheless able to self-organize into amyloid-like fibrils. This finding appears to render very promising the elastin-inspired biopolymers.

Acknowledgment. This work was supported by a European Community Project "ELAST − AGE" n. 018960". Thanks are due to Mr. Alessandro Laurita (CIM, Centre of Microscopy, University of Basilicata) for the ESEM micrograph. R.F. gratefully acknowledges Procter & Gamble IRC.

Supporting Information Available. HPLC chromatogram and electrospray mass spectrum of EX28 peptide. This material is available free of charge via the Internet at http://pubs.acs.org.

References and Notes

(1) Rosenbloom, J.; Abrams, W. R.; Mecham, R. *FASEB J.* **1993**, *7*, 1208−18.
(2) Castiglione Morelli, M. A.; DeBiasi, M.; DeStradis, A.; Tamburro, A. M. *J. Biomol. Struct. Dyn.* **1993**, *11*, 181−90.
(3) Tamburro, A. M.; Pepe, A.; Bochicchio, B.; Quaglino, D.; Ronchetti, I. P. *J. Biol. Chem.* **2005**, *280*, 2682−90.

(4) Miao, M.; Bellingham, C. M.; Stahl, R. J.; Sitarz, E. E.; Lane, C. J.; Keeley, F. W. *J. Biol. Chem.* **2003**, *278*, 48553−62.
(5) Flamia, R.; Salvi, A. M.; D'Alessio, L.; Castle, J. E.; Tamburro, A. M. *Biomacromolecules* **2007**, *8*, 128−38.
(6) Ostuni, A.; Bochicchio, B.; Armentano, F.; Bisaccia, F.; Tamburro, A. M. *Biophys. J.* **2007**, in press.
(7) Rodriguez-Cabello, J. C.; Prieto, S.; Reguera, J.; Arias, F. J.; Ribeiro, A. *J. Biomater. Sci. Polym. Ed.* **2007**, *18*, 269−86.
(8) Goeden-Wood, N. L.; Keasling, J. D.; Muller, S. J. *Macromolecules* **2003**, *36*, 2932−8.
(9) Davis, D. G.; Bax, A. *J. Am. Chem. Soc.* **1985**, *107*, 2820−1.
(10) Jeener, J.; Meier, B. H.; Bachmann, P.; Ernst, R. R. *J. Chem. Phys.* **1979**, *71*, 4546−53.
(11) Hwang, T. L.; Shaka, A. J. *J. Magn. Reson. Ser. A* **1995**, *112*, 275−9.
(12) Wüthrich, K. *NMR of Proteins and Nucleic Acids*; Wiley: New York, 1986.
(13) Bochicchio, B.; Tamburro, A. M. *Chirality* **2002**, *14*, 782−92.
(14) Tamburro, A. M.; Bochicchio, B.; Pepe, A. *Biochemistry* **2003**, *42*, 13347−62.
(15) Wishart, D. S.; Sykes, B. D.; Richards, F. M. *Biochemistry* **1992**, *31*, 1647−51.
(16) Urry, D. W.; Chang, D. K.; Krishna, N. R.; Huang, D. H.; Trapane, T. L.; Prasad, K. U. *Biopolymers* **1989**, *28*, 819−33.
(17) Jackson, M.; Mantsch, H. H. *Biochim. Biophys. Acta* **1991**, *1078*, 231−5.
(18) Martino, M.; Bavoso, A.; Guantieri, V.; Coviello, A.; Tamburro, A. M. *J. Mol. Struct.* **2000**, *519*, 173−89.
(19) Harris, P. I.; Chapman, D. *Biopolymers* **1995**, *37*, 251−63.
(20) Woody, R. W. *Adv. Biophys. Chem.* **1992**, *2*, 37−79.
(21) Surewicz, W. K.; Mantsch, H. H.; Chapman, D. *Biochemistry* **1993**, *32*, 389−94.
(22) Susi, H.; Timasheff, S. N.; Stevens, L. *J. Biol. Chem.* **1967**, *242*, 5460−6.
(23) Lefevre, T.; Arseneault, K.; Pezolet, M. *Biopolymers* **2004**, *73*, 705−15.
(24) Debelle, L.; Alix, A. J. *Biochimie* **1999**, *81*, 981−94.
(25) Chiti, F.; De Lorenzi, E.; Grossi, S.; Mangione, P.; Giorgetti, S.; Caccialanza, G.; Dobson, C. M.; Merlini, G.; Ramponi, G.; Bellotti, V. *J. Biol. Chem.* **2001**, *276*, 46714−21.
(26) Zurdo, J.; Guijarro, J. I.; Jimenez, J. L.; Saibil, H. R.; Dobson, C. M. *J. Mol. Biol.* **2001**, *311*, 325−40.
(27) Klunk, W. E.; Jacob, R. F.; Mason, R. P. *Methods Enzymol.* **1999**, *309*, 285−305.
(28) Mandelbrot, B. B. *The Fractal Geometry of Nature*; W. H. Freeman and Co.: New York, 1982.
(29) Tamburro, A. M.; De Stradis, A.; D'Alessio, L. *J. Biomol. Struct. Dyn.* **1995**, *12*, 1161−72.
(30) Martino, M.; Perri, T.; Tamburro, A. M. *Biomacromolecules* **2002**, *3*, 297−304.
(31) Ohgo, K.; Niemczura, W. P.; Ashida, J.; Okonogi, M.; Asakura, T.; Kumashiro, K. K. *Biomacromolecules* **2006**, *7*, 3306−10.
(32) Bochicchio, B.; Pepe, A.; Tamburro, A. M. *Matrix Biol.* **2001**, *20*, 243−50.
(33) DuBay, K. F.; Pawar, A. P.; Chiti, F.; Zurdo, J.; Dobson, C. M.; Vendruscolo, M. *J. Mol. Biol.* **2004**, *341*, 1317−26.
(34) Urry, D. W.; Starcher, B.; Partridge, S. M. *Nature* **1969**, *222*, 795−6.
(35) Vrhovski, B.; Jensen, S.; Weiss, A. S. *Eur. J. Biochem.* **1997**, *250*, 92−8.
(36) Bellingham, C. M.; Lillie, M. A.; Gosline, J. M.; Wright, G. M.; Starcher, B. C.; Bailey, A. J.; Woodhouse, K. A.; Keeley, F. W. *Biopolymers* **2003**, *70*, 445−55.
(37) Pepe, A.; Guerra, D.; Bochicchio, B.; Quaglino, D.; Gheduzzi, D.; Pasquali Ronchetti, I.; Tamburro, A. M. *Matrix Biol.* **2005**, *24*, 96−109.
(38) Rauscher, S.; Baud, S.; Miao, M.; Keeley, F. W.; Pomes, R. *Structure* **2006**, *14*, 1667−76.
(39) Bressan, G. M.; Castellani, I.; Giro, M. G.; Volpin, D.; Fornieri, C.; Pasquali Ronchetti, I. *J. Ultrastruct. Res.* **1983**, *82*, 335−40.
(40) Flamia, R.; Zhdan, P. A.; Martino, M.; Castle, J. E.; Tamburro, A. M. *Biomacromolecules* **2004**, *5*, 1511−8.

BM700636A